8

Crystallization of Water Mediated by Carbon

Tianshu Li, Yuanfei Bi, and Boxiao Cao

ABSTRACT

Carbon is known to influence the crystallization of water in different ways. By combining forward flux sampling method and molecular dynamics simulation, we successfully investigate the formation of ice and gas hydrate induced by carbon. Our study shows that although ice nucleation on graphitic carbon follows the pathway described by the classical nucleation theory, the molecular nucleation mechanisms are complex and strongly dependent on the characters of carbon surface, namely, chemistry, crystallinity, and topography. This behavior is thermodynamically simple but complex at the molecular scale, and is rationalized by the role of water ordering induced by carbon. On the other hand, small hydrocarbon molecules such as methane are known to induce the formation of clathrate hydrate. To this end, we find the nucleation of gas hydrate follows a nonclassical pathway in that an average hydrate nucleus is amorphous-like, but exhibits a free energy landscape that can be reasonably well described by classical nucleation theory. We attempt to rationalize this seeming contradictory by making an analogy between stacking disordering in ice nucleation and the random packing of cages in hydrate nucleation. This viewpoint thus allows potentially connecting the nucleation of ice and gas hydrate through a unified picture.

8.1. INTRODUCTION

Although crystallization of water appears quite ordinary in daily life, pure water is surprisingly difficult to freeze. For example, distilled water in a freezer can easily maintain its liquid state without transforming into ice for a very long time. In fact, pure water can be supercooled down to –35 °C, a temperature usually referred to as the homogeneous nucleation temperature, below which ice crystallization becomes inevitable. This seemingly counterintuitive phenomenon was first rationalized by Gibbs about 140 years ago (Gibbs, 1876, 1877): When a new phase becomes thermodynamically more stable than the parent phase, the formation of the new phase is driven by the chemical potential difference but hindered by the surface tension between the two phases. Because the resistance scales with the interfacial area while the driving force is proportional to the volume of the new phase, a barrier must be overcome before the growth of the new phase becomes energetically favorable. The insight was further developed into the well-known homogeneous classical nucleation theory (CNT) (Volmer & Weber, 1926), which has been frequently invoked to interpret both experimental and simulation results in nucleation study.

The fundamental reason that ice freezes near its equilibrium melting point is attributed to heterogeneous nucleation, an activation process that is mediated by impurities. These impurities, often termed ice nucleators (INs), generically exist in nature and encompass a vast variety of materials, spanning from mineral dusts to organic species (Murray et al., 2012). In fact, the crystallization of nearly all materials proceeds via heterogeneous nucleation. The prevalence of heterogeneous nucleation in nature can be explained qualitatively by the extension of the CNT, which was established more than 60 years ago (Turnbull, 1950). The theory attributes the

Department of Civil and Environmental Engineering, George Washington University, Washington, DC, USA

Carbon in Earth's Interior, Geophysical Monograph 249, First Edition. Edited by Craig E. Manning, Jung-Fu Lin, and Wendy L. Mao.

enhanced nucleation rate to the reduced nucleation barrier due to the presence of a heterogeneous interface between liquid and substrate. Although the theory is well known, its quantitative validity and key conclusions have remained unconfirmed. In fact, criticisms have often been drawn towards its assumptions and quantitative validity (Gebauer & Cölfen, 2011; Sear, 2012). In complex systems, e.g., minerals, proteins, organic crystals, and hydrates, the crystallization process is often found to proceed in a multistep, nonclassical fashion (Chen et al., 2011; Erdemir et al., 2009; Gebauer & Cölfen, 2011; Gebauer et al., 2008; Jacobson et al., 2010; Vekilov, 2004). Even in simple systems such as colloids, the nucleation behaviors are often found to deviate from CNT (Auer & Frenkel, 2003).

It may seem rather unusual to relate carbon to the liquid-to-solid transformation of water, as in its first look, there appears to be a lack of apparent structural similarity between the two. Nevertheless, the crystallization of water is known to be strongly affected by the presence of carbon through a variety of forms. Many carbon-bearing materials are known to be effective INs in atmosphere, e.g., soot particles and organic compounds. In particular, graphitic carbon has been long conjectured to influence ice formation, but its role has not been clearly elucidated. In the deep ocean, small hydrocarbon molecules such as methane are known to trigger the crystallization of water into clathrate hydrate, another form of solid water.

In this chapter, we review our recent studies on the crystallization of water induced by carbon by using advanced molecular simulations. In particular, we attempt to answer the following fundamental questions: How is the crystallization of water initiated and controlled by the fundamental level interaction between carbon and water? Can we combine the two distinct processes within a unified framework? To address these questions, we employed advanced sampling method combined with molecular simulations to investigate the nucleation of ice and gas hydrate in the presence of carbon-bearing materials.

8.2. METHODS

The main challenge in modeling nucleation is to overcome the long induction time of the event, which significantly exceeds the accessible time scale of direct molecular simulation, i.e., nanosecond to microsecond. For example, a typically measured ice nucleation rate in experiment (e.g., 10^9 $cm^{-3}s^{-1}$) requires a trajectory as long as ~32 years to reproduce in a direct molecular dynamics (MD) simulation employing a simulation volume of 1000 nm^3. To overcome this shortcoming, we employed forward flux sampling (FFS) method (Allen et al., 2006) to accelerate the exploration of transition pathways between disordered (liquid) and ordered (crystal) states.

In this approach, the nucleation trajectory is decomposed into a series of consecutive transition segments through an appropriate order parameter λ. The rate constant is obtained using the "effective positive flux" expression (van Erp et al., 2003) $R_{AB} = \Phi_{\lambda_0} p(\lambda_B|\lambda_0)$, where Φ_{λ_0} is the flux rate reaching the first interface λ_0 from basin A (liquid), and $P(\lambda_B|\lambda_0)$ is the probability for a trajectory that starts from λ_0 and eventually reaches B (solid). The typically small $P(\lambda_B|\lambda_0)$ can be calculated through $P(\lambda_B|\lambda_0) = \prod_{i=1}^{n} P(\lambda_i|\lambda_{i-1})$, where $P(\lambda_i|\lambda_{i-1})$ is the crossing probability between the two adjacent interfaces λ_{i-1} and λ_i. Although FFS ensures R_{AB} is independent of the exact positions of interfaces, we find it optimal to choose λ_is that yield $P(\lambda_i|\lambda_{i-1})$ within the range of 0.01–0.2, to balance between computational efficiency and statistical variance (Li et al., 2009). Through combining FFS and backward flux sampling (BFS), one can also obtain the free energy profile along a sequence of order parameter (Bi, Porras, et al., 2016; Valeriani et al., 2007). For ice nucleation, we use the number of ice-like water molecules, which are characterized by local bond-order parameter q_6 (Li et al., 2011), in the largest crystallite as an effective order parameter; for gas hydrate, we have developed the half-cage order parameter on the basis of structural signature of clathrate (Bi & Li, 2014). The choice of both order parameters can be justified by p_B-histogram analyses (Bi, Porras, et al., 2016; Cabriolu & Li, 2015; DeFever & Sarupria, 2017; Lupi et al., 2016) that show both order parameters describe well the nucleation pathways of ice and hydrate.

8.3. HETEROGENEOUS ICE NUCLEATION FACILITATED BY GRAPHITIC CARBON

8.3.1. Verification of Heterogeneous Classical Nucleation Theory

We began our investigation by first examining ice nucleation on graphitic carbon. Water is represented by the monoatomic water model mW (Molinero & Moore, 2009), while the water-carbon interaction is described by the two-body term of the mW, where ε and σ are reparametrized to reproduce the experimental contact angle (86°) of water on graphite Lupi et al., 2014). The foremost question to address is whether CNT can describe heterogeneous ice nucleation, because although CNT has been routinely invoked to explain both experimental and simulation results, its quantitative applicability in ice nucleation remains unknown. A verification of CNT requires obtaining the key quantities (e.g., nucleation rate, critical nucleus size) independent of theory, which is challenging for both experiment and simulation. The capability of obtaining an ice nucleation rate independent

of CNT by FFS allows testing the quantitative validity of the theory in heterogeneous ice nucleation for the first time.

The nucleation rates of ice forming homogeneously from supercooled water (Li et al., 2011) and heterogeneously on a graphene surface (Cabriolu & Li, 2015) are computed as a function of temperature. As shown in Figure 8.1, the computed ice nucleation rates were found to fit well according to CNT through the expression $\ln R = \ln A + C/((T - T_m)^2 T)$. Here, R, T, and T_m are the rate constant, nucleation temperature, and melting temperature of ice, respectively, while A and C are fitting constants. The fitting procedure yields the estimate of the potency factor, which measures the ratio of the barrier of heterogeneous nucleation to that of homogeneous nucleation, *i.e.*, $f(\theta) \equiv \Delta G^*_{het}/\Delta G^*_{\mathrm{hom}} = C_{het}/C_{\mathrm{hom}}$, directly through the fitting constant C.

On the other hand, the critical volume (or the critical size λ^*) can also be independently obtained from the ensemble of nucleation trajectories obtained in FFS calculation, using the definition of committor (Bolhuis et al., 2002) $p_B = 0.5$, *i.e.*, the critical nucleus should have the equal probabilities of dissolving and growing completely. On the basis of CNT, we can fit the obtained critical size as a function of temperature through $\lambda = B/(T_m/T - 1)^3$. Again, an excellent fitting is obtained (Figure 8.1c), from which one can obtain the volumetric ratio $\lambda^*_{het}/\lambda^*_{\mathrm{hom}} = B_{het}/B_{\mathrm{hom}}$.

Remarkably, the obtained volumetric ratio $B_{het}/B_{hom} = 0.480 \pm 0.011$ agrees quantitatively with the potency factor $C_{het}/C_{hom} = 0.456 \pm 0.019$. To ensure the agreement is not incidental, we also tested our conclusion at a different potency factor $f(\theta)$, through reducing the water-carbon interaction strength ε by one half so that the carbon surface now becomes more hydrophobic. We repeated the above procedures, and again obtained a quantitative agreement (Figure 8.1). To the best of our knowledge, this is the first time that the quantitative power of heterogeneous CNT has been directly supported from the independent rate constant calculation.

It should be mentioned that the quantitative equivalency between the volumetric factor and potency factor was again identified in our very recent study of ice nucleation on kaolinite surface (Sosso et al., 2016). The agreement with CNT, identified in different systems, is surely a strong support to the theory developed many decades ago, but it also raises an important question: behind this seemingly "simple" process, what determines the potency factor at the molecular level? Indeed, this has been one of the daunting questions in atmospheric chemistry for decades (Murray et al., 2012), as no strong correlation seems to exist between any of the proposed empirical criteria and the observed ice nucleation efficiency.

8.3.2. Molecular Insight Into the Complex Nature of Heterogeneous Ice Nucleation

To illustrate the molecular origin for the lack of such correlation, we examine the roles of surface crystallinity, surface hydrophilicity (Bi, Cabriolu, et al., 2016), and surface geometry (Bi et al., 2017) on ice nucleation based on the carbon-water system. We introduce Stone-Wales defects in crystalline graphene through applying the Wooten-Weaire-Winer bond-switching Monte-Carlo method (Wooten et al., 1985) to mimic the change of surface crystallinity. The resulting amorphous graphene is shown in Figure 8.2. To tune surface hydrophilicity, we modify water-carbon interaction strength ε in the wide range of $[\varepsilon_0, 10\varepsilon_0]$, where ε_0 is the original strength (Lupi et al., 2014) reproducing the water contact angle (86°) on graphite (Li & Zeng, 2012). Increasing water-carbon interaction strength makes the surface more hydrophilic (Lupi & Molinero, 2014), as carbon atoms bind water more strongly. To understand the role of surface roughness, we also create an atomically sharp wedge composed of two graphene planes with a varying wedge angle β.

We found that heterogeneous ice nucleation on a flat graphitic surface exhibits a rich spectrum of nucleation behaviors when both surface crystallinity and surface hydrophilicity were allowed to vary (Bi, Cabriolu, et al., 2016). As shown in Figure 8.2, a radical change in surface chemistry not only yields a nonmonotonic change in ice nucleation rates, but it also leads to a complex, alternate nucleation mechanism: At a low water-carbon strength (i.e., low hydrophilicity), ice nucleation is found to be mainly controlled by the hydrophilicity of carbon alone, thus independent of the crystallinity of the graphene substrate. A gradual increase of hydrophilicity is then found to differentiate between crystalline and amorphous graphene, with crystalline graphene being distinguished as a more efficient IN. Interestingly, a further increase of hydrophilicity not only leads to a sudden decrease of the nucleation rate, but also eliminates the role of crystallinity in nucleation, making ice nucleation behavior similar to what occurs at low hydrophilicity. Remarkably, with a very high surface hydrophilicity, the coupling-controlled behavior reappears so that the crystalline graphene again becomes a better IN. Such oscillating distinction between crystalline and amorphous graphene in their ice nucleation efficiencies clearly highlights the complexity of heterogeneous ice nucleation and suggests that ice nucleation can be controlled by the combined surface characteristics via coupling effects.

Similarly, we also found that surface geometry alone cannot be a good descriptor for ice nucleation efficiency either. Although surface roughness has been generally considered as a favorable factor for nucleation, our study (Bi et al., 2017) showed that a simple correlation cannot

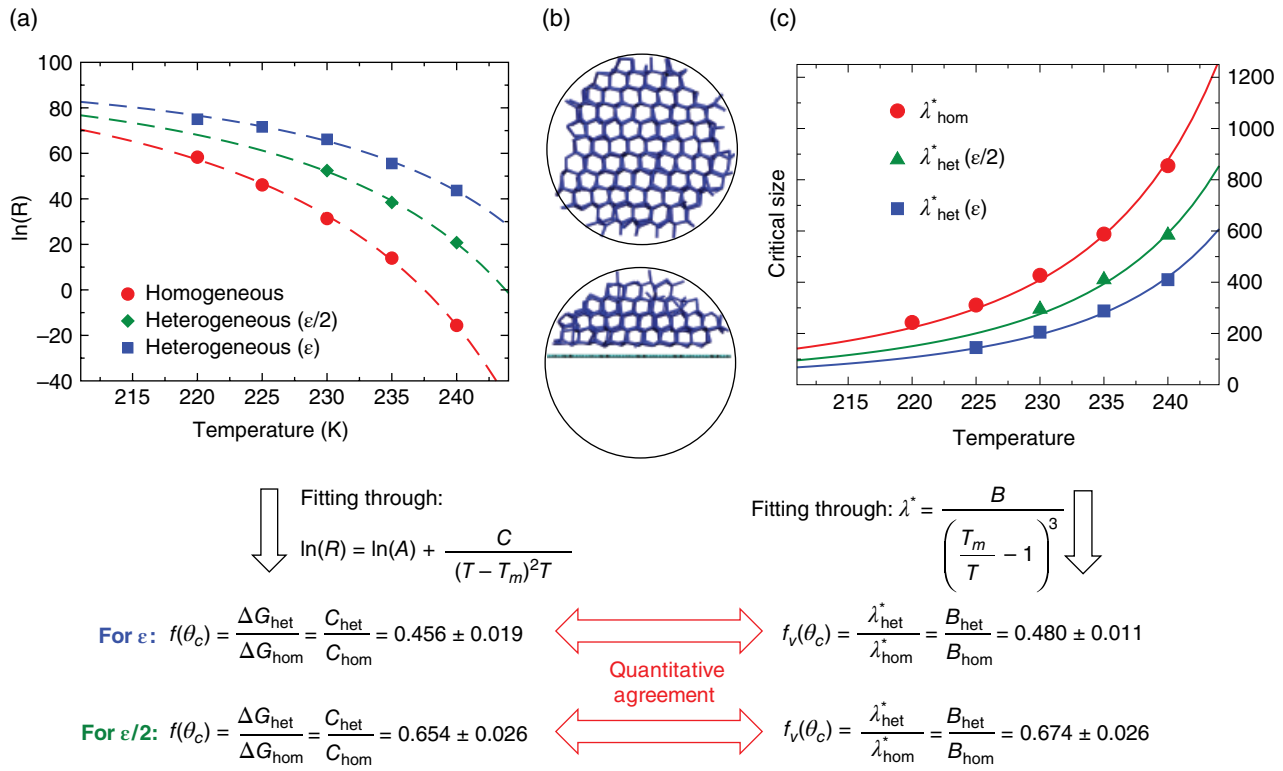

Figure 8.1 The variation of (a) the calculated ice nucleation rate (logarithm) and (c) critical size, with temperature. Data on homogeneous ice nucleation are from our previous work (Li et al., 2011). Reproduced by permission of the PCCP Owner Societies. (b) Snapshots of the critical ice nuclei for homogenous and heterogeneous nucleation at 240 K. *Source*: Cabriolu & Li (2015) Reproduced with permission of the American Physical Society. Copyright (2019) American Physical Society. See electronic version for color representation of the figures in this book.

be established between surface geometry and ice nucleation efficiency. As shown in Figure 8.3, the calculated nucleation rates of ice forming within a concave, atomically sharp wedge showed a nonmonotonic dependence on the wedge angle. In particular, the significant enhancement of ice nucleation relative to a planar surface was found to occur only under a few well-defined wedge angles: 70°, 110°, and 45°. Our studies thus suggested that it is unlikely that a single descriptor can reliably determine an IN's efficiency, and a thorough understanding of the ice nucleation capacity for an IN therefore should be achieved through a comprehensive study that explicitly considers all the necessary molecular details at the surface.

8.3.3. Role of Local Ordering of Water in Ice Nucleation

To understand this "duality" of ice nucleation, i.e., being thermodynamically "simple" but complex at molecular scales, we examine the local ordering of interfacial water. Indeed, we find the observed complex heterogenous ice nucleation behaviors can be generally interpreted based on this concept regardless of the diversity in surface character. Specifically, for ice nucleation on a flat graphene surface (Figure 8.2), we find a simple trend behind the complex ice nucleation behaviors: The better ice nucleation efficiency of crystalline graphene, whenever it occurs, is always accompanied by the appearance of *lattice registry* between ice and crystalline graphene, whether such registry occurs in the first or second contact layer of water. Further investigation shows that the occurrence of lattice registry is a direct outcome of in-plane water ordering as a result of the subtle balance between water-carbon binding strength and lattice mismatch between graphene and ice lattice.

The concept of local ordering can be also applied to explain the enhanced ice nucleation via a special surface geometry (Bi et al., 2017). Because graphene induces density layering of water that matches the density profile of ice normal to its basal plane (Lupi et al., 2014), it promotes the formation of the {0001} plane of hexagonal ice I_h or the {111} plane of cubic ice I_c. This one-dimensional density match alone leads to an enhancement of the ice nucleation rate by 25 orders of magnitude at 240 K. When two graphene planes intersect at 70°/110°, forming a wedge, they create a template that matches *two* intersecting {111} planes of cubic I_c simultaneously, which

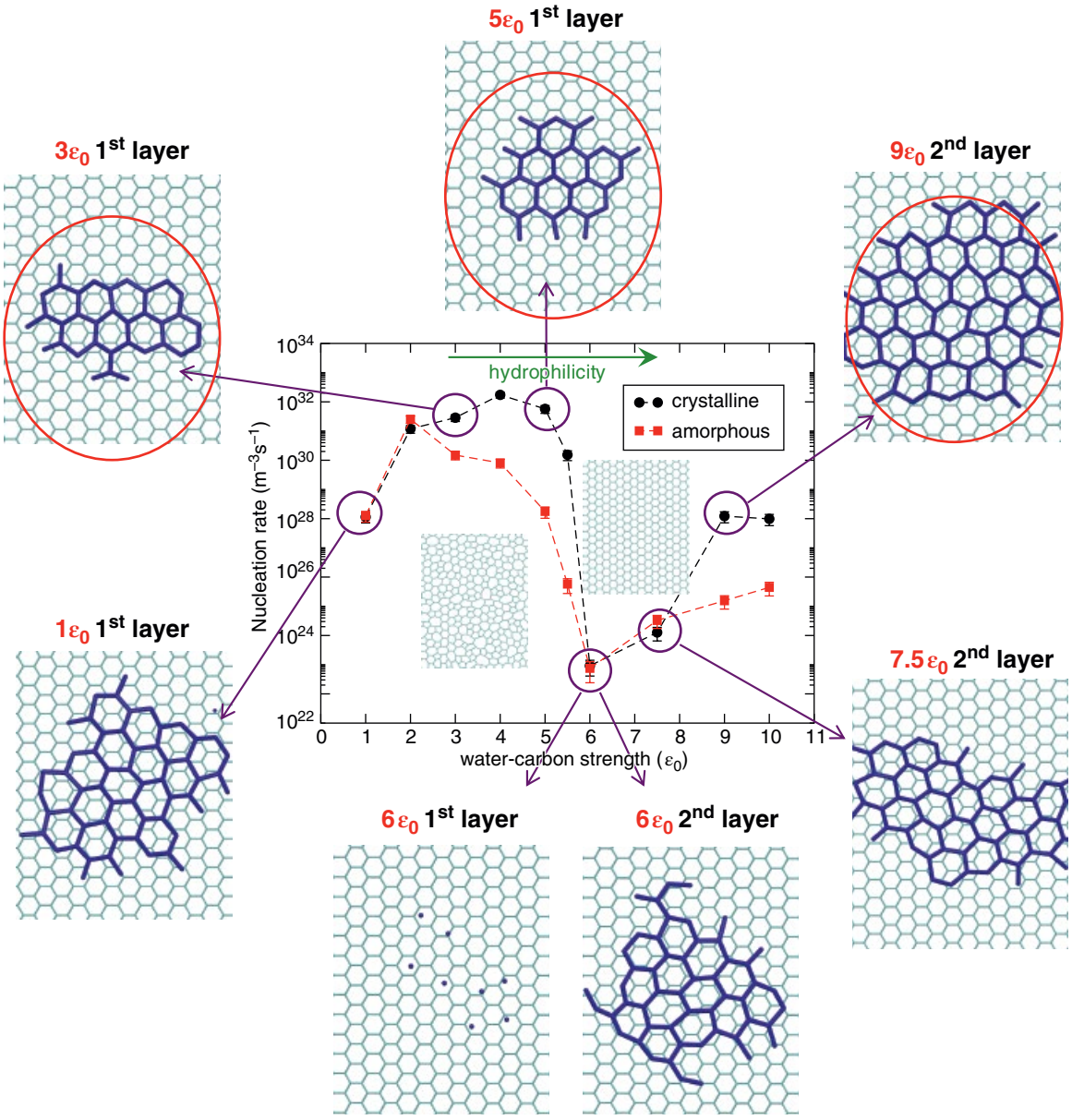

Figure 8.2 Variation of ice nucleation rates with water-carbon strength for both crystalline and amorphous graphene at 230 K. Inset: Structure of the crystalline and amorphous graphene. The panels show the structures of ice (blue) forming in the contact layers of water above graphene substrate (cyan) at different ε. Red circles highlight the ice basal plane registered with the underlying crystalline graphene lattice. *Source*: Bi, Cabriolu, et al. (2016). Reproduced with permission of the American Chemical Society. Copyright (2019) American Chemical Society. See electronic version for color representation of the figures in this book.

further enhances the ice nucleation rate by another eight orders of magnitude. Similarly, adding a third graphene sheet while creating an open tetrahedral pyramid that matches three intersecting {111} planes was found to yield spontaneous ice nucleation. It is also important to note that the increasing degree of induced ordering not only enhances the nucleation rate but also leads to an interesting enhancement of polymorph selection toward cubic ice I_c.

Importantly, we find the ordering of liquid that pertains to crystallization is not limited to apparent lattice match. In particular, noting that a 45° wedge does not accommodate any common crystalline dihedral angle, we find that the very high ice nucleation efficiency of the 45° wedge must not be explained based on the traditional wisdom of lattice match. Instead, we find that such unexpected rate enhancement is facilitated by the formation of special *topological defects* near the 45° wedge tip that

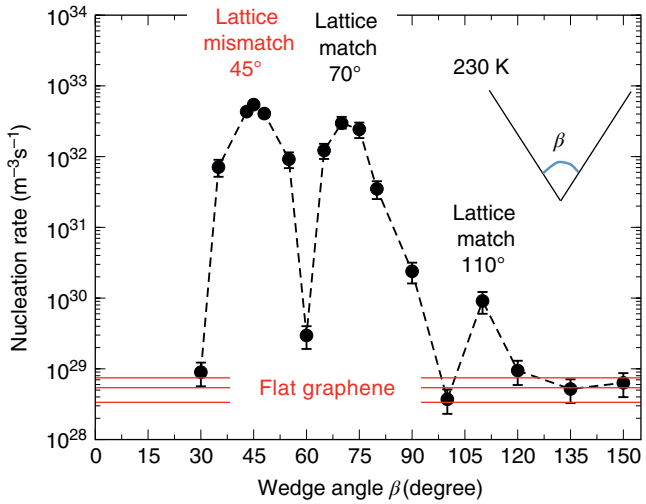

Figure 8.3 Variation of the calculated nucleation rates of ice forming within an atomically sharp, concave wedge. *Source*: Bi et al. (2017). Reproduced with permission of Nature Communications. See electronic version for color representation of the figures in this book.

consequently catalyze the growth of regular ice (Figure 8.4). The close resemblance in the molecular pathways for ice to form within the 70° wedge (Figure 8.4 g–i, nondefect initiating) and 45° wedge (Figure 8.4 c–e, defect initiating), along with their nearly degenerate ice nucleation rates (Figure 8.3), highlight the strong relevance of defects in ice nucleation. Therefore, we believe that the traditional concept of structural match or templating effect in nucleation should be extended to include a broader structural match with *noncrystalline* units.

The local ordering of liquid can naturally reconcile the duality of heterogeneous ice nucleation. From a thermodynamic viewpoint, since crystallization is driven by enthalpy gain but penalized by entropy loss, there must exist a critical point prior to which the enthalpy gain cannot be fully compensated by entropy loss. This critical point should be conceptually equivalent to the nucleation barrier in CNT. Therefore, a crystallization event can be enhanced when entropy loss is mitigated. At a molecular level, such reduction of entropy loss is reflected by the enhancement of local ordering of liquid in consistent

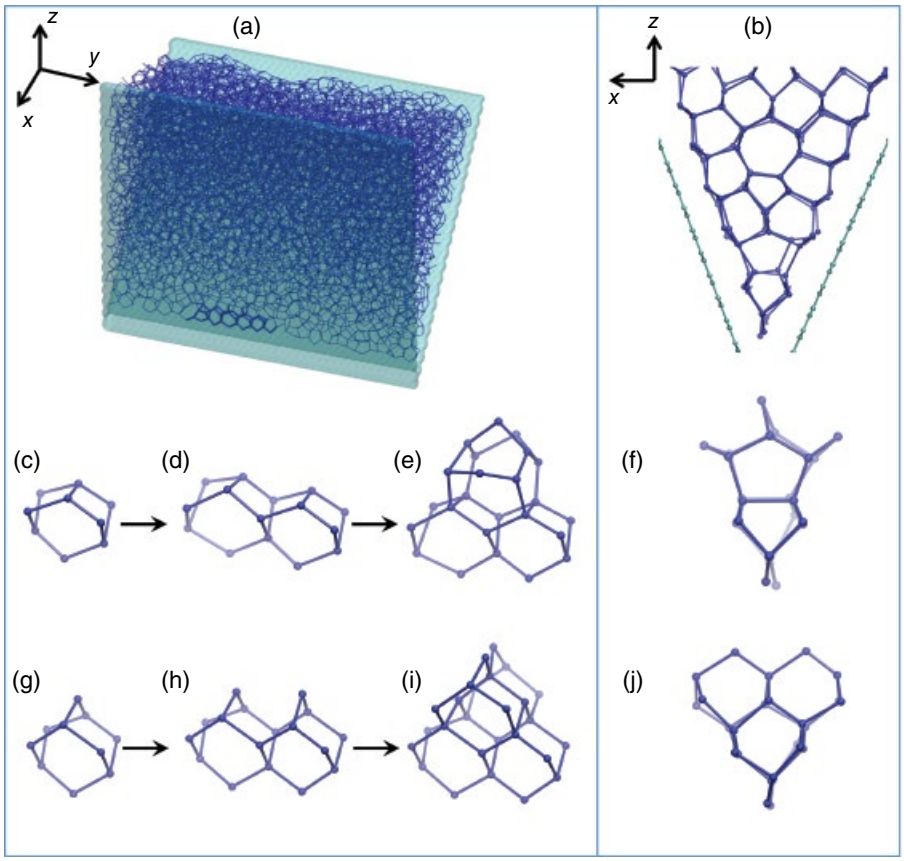

Figure 8.4 Molecular pathways of ice crystallization near tip of a 45° wedge (c–e) and a 70° wedge (g–i). (b), (f), and (j) are the side views of (a), (e), and (i), respectively. *Source*: Bi et al. (2017). Reproduced with permission of Nature Communications. See electronic version for color representation of the figures in this book.

with crystallization, which can be facilitated by certain characteristics of an IN, e.g., surface chemistry, surface crystallinity, surface geometry, etc. In this sense, the role of an IN is to "guide" water molecules to find the right entrance towards the basin of solid phase.

8.4. NUCLEATION OF GAS HYDRATE

Another major venue for water crystallization induced by carbon is the formation of gas hydrate. Small hydrocarbon molecules such as methane are known to be capable of inducing water to crystallize into clathrate structures, enclosing them as guests under high pressure. These carbon-bearing molecules, being strongly hydrophobic, have very low solubilities in water, yet their concentrations can be thousand times higher in solid gas hydrate. Although appearing chemically counterintuitive, the formation of gas hydrate can be well rationalized by both thermodynamics and kinetics. On one hand, the presence of many pairs of gas-water interaction can significantly stabilize gas hydrates, making their formation thermodynamically favorable; on the other, the close resemblance in water's structure between the hydration shell of gas molecule and clathrate cage provides a structural basis for gas hydrate nucleation. Despite these understandings, an outstanding question is how gas hydrate nucleates from liquid-gas mixture, and in particular, whether hydrate nucleation pathways can be described by CNT. Early hypotheses such as labile cluster hypothesis (LCH) (Sloan & Fleyfel, 1991) and local structuring hypothesis (LSH) (Radhakrishnan & Trout, 2002) were able to rationalize certain attributes of hydrate nucleation mechanism, but both found difficulty when compared with simulation results. The breakthrough was made when spontaneous hydrate nucleation was for the first time obtained in direct MD simulations (Walsh et al., 2009). These simulations facilitated a new view of hydrate nucleation: "blob" mechanism (Jacobson & Molinero, 2010), which reconciles labile cluster hypothesis and local structuring hypothesis. In particular, the "blob" mechanism makes an analogy between hydrate nucleation and the nucleation of minerals and protein, suggesting a "two-step" process involving the formation of amorphous nucleus followed by amorphous-to-crystal transition. The mechanism raised a fundamental question of whether hydrate nucleation can be considered nonclassical with multiple barriers, as hypothesized in the nucleation of proteins and minerals.

An unambiguous answer to this question requires a sufficient sampling of transition pathway ensemble as well as a determination of free energy profile along the transition pathway. To achieve this goal, we developed the half-cage order parameter (H-COP) (Bi & Li, 2014) on the basis of the topological hierarchy of clathrate structure (see Figure 8.5a), for driving and characterizing hydrate nucleation. H-COP is defined as the number of water molecules contained in a hydrate-like cluster assembled by half cages through certain geometrical constraints. We subsequently integrated H-COP into FFS, which allows explicitly computing hydrate nucleation rate for the first time at a condition where spontaneous hydrate nucleation is too slow to occur in direct MD simulation (Bi & Li, 2014). Combining FFS and backward flux sampling also allowed obtaining the free energy profile of hydrate nucleation along the order parameter H-COP (Bi, Porras, et al., 2016). Our study of gas hydrate nucleation was carried out based on a coarse-grained model where water is represented by the mW model and water-gas interactions are represented by the two-body interaction of the mW model (Jacobson & Molinero, 2010) that was tuned to mimic a wide range of guests with different sizes and solubilities (Jacobson et al., 2010). In this study we considered both a large (L) guest that exhibits properties comparable to oxetane and a medium (M) guest that emulates methane.

Our investigation demonstrates a few important and intriguing characteristics of gas hydrate nucleation: (1) The ensemble-averaged crystallinity of hydrate is found to be low at the early stage of nucleation but gradually increases with the size of the hydrate nucleus, thus providing a strong support to the proposed "two-step" nucleation mechanism. (2) Despite the average two-step picture, there clearly exists a structural diversity of hydrate nucleation pathway. In particular, multiple nucleation channels are shown to exist, among which hydrate is found to form directly into a crystalline structure, bypassing the amorphous stage. (3) Most surprisingly, the free energy profile of hydrate nucleation is found to follow CNT reasonably well, despite the overall "nonclassical" molecular pathways.

These observations appear contradictory, particularly (1) and (3). However, our subsequent investigation showed they may be reconciled by considering the following facts and hypotheses. First, the chemical potential difference between structure I (sI) hydrate, which is the thermodynamically stable phase of the studied gas hydrate, and the metastable phase structure II (sII) hydrate, is very small. The close proximity of structural stability in sI and sII is reminiscent of the case of ice I, where hexagonal I_h is only marginally more stable than cubic I_c. For ice, both simulations (Haji-Akbari & Debenedetti, 2015; Li et al., 2011; Moore & Molinero, 2011) and experiments (Kuhs et al., 2012; Malkin et al., 2012) have shown ice crystallites grown freshly from supercooled water are stacking disordered, rather than pure I_h or I_c. This unconventional behavior has been recently rationalized by the higher stability of stacking disordered ice crystallites,

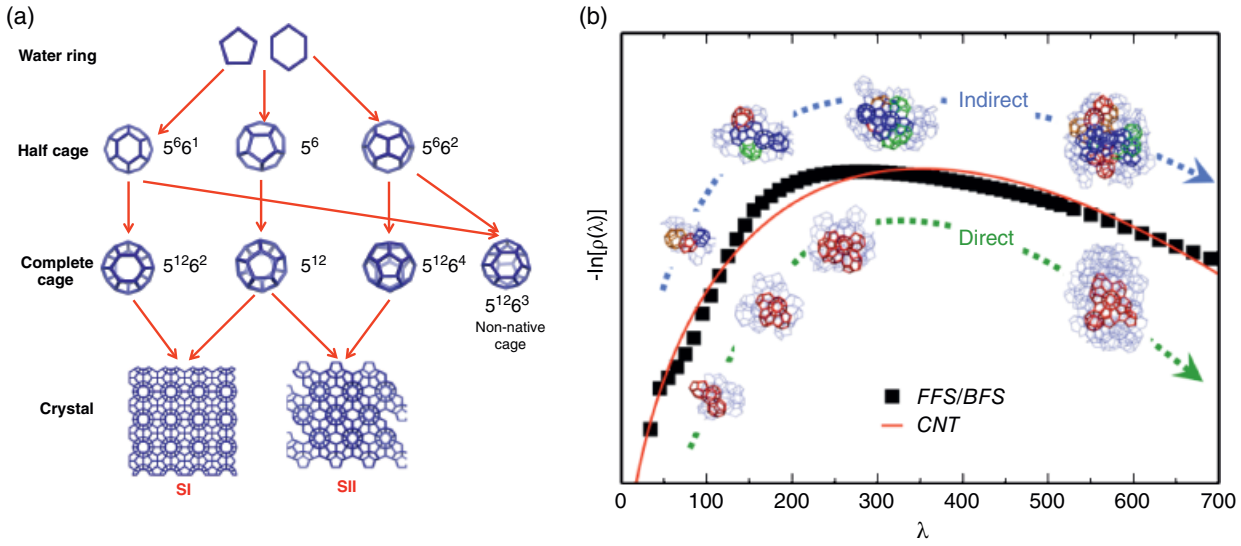

Figure 8.5 (a) Topological hierarchy of clathrate hydrate. (b) Calculated free energy profile for L-hydrate nucleation as a function of order parameter. Red line represents the best fit of classical nucleation theory. Both direct and indirect pathways are hypothesized to exhibit similar energy landscape. For indirect pathway, the color scheme for complete cages is 512 (blue), 51262 (red), 51263 (green), and 51264 (orange); for direct pathway, the sII-like hydrate cages are marked red. *Source*: Bi, Porras, et al. (2016). Reproduced with permission of AIP Publishing. See electronic version for color representation of the figures in this book.

as a result of entropy of mixing thermodynamically favoring stacking disorder (Lupi et al., 2017). From this viewpoint, we postulate that hydrate nucleation may be rationalized by a similar argument, as the close stability in the large variety of cage packing sequences guarantees a large configurational space for hydrate nucleation to explore (Hall et al., 2016). Since crystalline structures only represent a small fraction of such large configurational space (as they are outnumbered by noncrystalline packing sequences, just as stacking ordered structures are outnumbered by stacking disordered structures), the entropy of "mixing" favors a random packing of cages, thus forming noncrystalline hydrate nucleus. As a result, hydrate nuclei exhibit a wide range of crystallinity, and the ensemble-averaged crystallinity is low for small hydrate nucleus. As explained in the section above, classical nucleation theory has been shown to describe ice nucleation accurately—even when stacking disorder is considered (Lupi et al., 2017). In this sense, it is then not too surprising to find that hydrate nucleation also carries a classical-like free energy profile, albeit that small deviation is observed between the calculation and the fitting (see Figure 8.5b). One explanation for such deviation could be related to the choice of order parameter: As shown in a recent study (DeFever & Sarupria, 2017), although all the developed order parameters for hydrate nucleation, including H-COP, capture the reaction pathway well, they are in general less accurate than that for ice nucleation.

8.5. CONCLUSION

An intriguing question to address is how the crystallization of water is initiated and controlled by the fundamental level interaction between carbon and water. By developing advanced molecular modeling, we address this question at both the thermodynamic and molecular levels. We find ice crystallization, when either occurring homogeneously or heterogeneously on a graphitic carbon surface, appears to follow a pathway that can be quantitatively described by classical nucleation theory. On the other hand, at a molecular level, we also discover that ice nucleation is dictated by the subtle interplay between different molecular details of the carbon surface, including surface crystallinity, surface hydrophilicity, and surface topography. We attempt to explain this duality of ice nucleation through the role of local ordering of water. In the form of small hydrocarbons such as methane, carbon can also directly participate in the crystallization of water, leading to the formation of clathrate hydrate. To this end, by using our developed tools, we find that although on average, hydrate nucleation proceeds through a nonclassical pathway, it displays a classical-like free energy profile. We attempt to reconcile this seeming contradiction through making an analogy between the stacking disorder in ice nucleation and the random packing of cages in hydrate nucleation. This analogy potentially allows understanding the crystallization of water through a unified framework, irrespective of its end products.

ACKNOWLEDGMENTS

The work has been supported by the Sloan Foundation through the Deep Carbon Observatory, NSF through awards CMMI-1537286 and CBET-1264438, and the American Chemical Society Petroleum Research Fund.

REFERENCES

Allen, R. J., Frenkel, D., Wolde, & Ten, P. R. (2006). Simulating rare events in equilibrium or nonequilibrium stochastic systems. *J Chem Phys*, *124*(2), 024102.

Auer, S., & Frenkel, D. (2003). Line tension controls wall-induced crystal nucleation in hard-sphere colloids. *Phys Rev Lett*, *91*(1), 015703.

Bi, Y., Cabriolu, R., & Li, T. (2016). heterogeneous ice nucleation controlled by the coupling of surface crystallinity and surface hydrophilicity. *J Phys Chem C*, *120*(3), 1507–1514.

Bi, Y., Cao, B., & Li, T. (2017). Enhanced heterogeneous ice nucleation by special surface geometry. *Nat Commun*, *8*, 15372.

Bi, Y., & Li, T. (2014). Probing methane hydrate nucleation through the forward flux sampling method. *J Phys Chem B*, *118*(47), 13324–13332.

Bi, Y., Porras, A., & Li, T. (2016). Free energy landscape and molecular pathways of gas hydrate nucleation. *J Chem Phys*, *145*(21), 211909.

Bolhuis, P. G., Chandler, D., Dellago, C., & Geissler, P. L. (2002). Transition path sampling: Throwing ropes over rough mountain passes, in the dark. *Annu. Rev. Phys. Chem.*, *53*, 291–318.

Cabriolu, R., & Li, T. (2015). Ice nucleation on carbon surface supports the classical theory for heterogeneous nucleation. *Physical Review E*, *91*, 052402.

Chen, J., Sarma, B., Evans, J. M. B., & Myerson, A. S. (2011). Pharmaceutical crystallization. *Crystal Growth & Design*, *11*(4), 887–895.

DeFever, R. S., Sarupria, S. (2017). Nucleation mechanism of clathrate hydrates of water-soluble guest molecules. *J Chem Phys*, *147*(20), 204503.

Erdemir, D., Lee, A. Y., & Myerson, A. S. (2009). Nucleation of crystals from solution: Classical and two-step models. *Acc. Chem. Res.*, *42*(5), 621–629.

Gebauer, D., & Cölfen, H. (2011). Prenucleation clusters and non-classical nucleation. *Nano Today*, *6*(6), 564–584.

Gebauer, D., Volkel, A., & Cölfen, H. (2008). Stable prenucleation calcium carbonate clusters. *Science*, *322*(5909), 1819–1822.

Gibbs, J. W. (1876). On the equilibrium of heterogeneous substances. *Transactions of the Connecticut Academy of Arts and Sciences*, *3*, 108–248.

Gibbs, J. W. (1877). On the equilibrium of heterogeneous substances. *Transactions of the Connecticut Academy of Arts and Sciences*, *3*, 343–524.

Haji-Akbari, A., & Debenedetti, P. G. (2015). Direct calculation of ice homogeneous nucleation rate for a molecular model of water. *Proc Natl Acad Sci USA*, *112*(34), 10582–10588.

Hall, K. W., Carpendale, S., & Kusalik, P. G. (2016). Evidence from mixed hydrate nucleation for a funnel model of crystallization. *Proceedings of the National Academy of Sciences*, 201610437.

Jacobson, L. C., Hujo, W., & Molinero, V. (2010a). Amorphous precursors in the nucleation of clathrate hydrates. *J Am Chem Soc*, *132*(33), 11806–11811.

Jacobson, L. C., Hujo, W., & Molinero, V. (2010b). Nucleation pathways of clathrate hydrates: Effect of guest size and solubility. *J Phys Chem B*, *114*(43), 13796–13807.

Jacobson, L. C., & Molinero, V. A (2010). Methane-water model for coarse-grained simulations of solutions and clathrate hydrates. *J Phys Chem B*, *114* (21), 7302–7311.

Kuhs, W. F., Sippel, C., Falenty, A., & Hansen, T. C. (2012). Extent and relevance of stacking disorder in "ice Ic." *Proceedings of the National Academy of Sciences*, *109*(52), 21259–21264.

Li, H., & Zeng, X. C. (2012). Wetting and interfacial properties of water nanodroplets in contact with graphene and monolayer boron-nitride sheets. *ACS Nano*, *6*(3), 2401–2409.

Li, T., Donadio, D., & Galli, G. (2009). Nucleation of tetrahedral solids: A molecular dynamics study of supercooled liquid silicon. *J. Chem. Phys.*, *131*(22), 224519.

Li, T., Donadio, D., Russo, G., & Galli, G. (2011). Homogeneous ice nucleation from supercooled water. *Phys Chem Chem Phys*, *13*(44), 19807–19813.

Lupi, L., Hudait, A., & Molinero, V. (2014). Heterogeneous nucleation of ice on carbon surfaces. *J Am Chem Soc*, *136*(8), 3156–3164.

Lupi, L., Hudait, A., Peters, B., Grünwald, M., Mullen, R. G., Nguyen, A. H., & Molinero, V. (2017). Role of stacking disorder in ice nucleation. *Nature*, *551*(7679), 218–222.

Lupi, L., & Molinero, V. (2014). Does hydrophilicity of carbon particles improve their ice nucleation ability? *J Phys Chem A*, *118*(35), 7330–7337.

Lupi, L., Peters, B., & Molinero, V. (2016). Pre-ordering of interfacial water in the pathway of heterogeneous ice nucleation does not lead to a two-step crystallization mechanism. *J Chem Phys*, *145*(21), 211910.

Malkin, T. L., Murray, B. J., Brukhno, A. V., Anwar, J., & Salzmann, C. G. (2012). Structure of ice crystallized from supercooled water. *Proceedings of the National Academy of Sciences*, *109*(4), 1041–1045.

Molinero, V., & Moore, E. B. (2009). Water modeled as an intermediate element between carbon and silicon. *J Phys Chem B*, *113*(13), 4008–4016.

Moore, E. B., & Molinero, V. (2011). Is it cubic? Ice crystallization from deeply supercooled water. *Phys Chem Chem Phys*, *13*(44), 20008–20016.

Murray, B. J., O'Sullivan, D., Atkinson, J. D., & Webb, M. E. (2012). Ice nucleation by particles immersed in supercooled cloud droplets. *Chem. Soc. Rev.*, *41*(19), 6519–6554.

Radhakrishnan, R., & Trout, B. (2002). A new approach for studying nucleation phenomena using molecular simulations: Application to CO2 hydrate clathrates. *J Chem Phys*, *117*(4), 1786–1796.

Sear, R. P. (2012). The non-classical nucleation of crystals: Microscopic mechanisms and applications to molecular

crystals, ice and calcium carbonate. *International Materials Reviews*, *57*(6), 328–356.

Sloan, E., & Fleyfel, F. A (1991). Molecular mechanism for gas hydrate nucleation from ice. *AIChE Journal*, *37*, 1281–1292.

Sosso, G. C., Li, T., Donadio, D., Tribello, G. A., & Michaelides, A. (2016). Microscopic mechanism and kinetics of ice formation at complex interfaces: Zooming in on kaolinite. *J Phys Chem Lett*, *7*, 2350–2355.

Turnbull, D. (1950). Kinetics of heterogeneous nucleation. *J Chem Phys*, *18*(2), 198.

Valeriani, C., Allen, R. J., Morelli, M. J., Frenkel, D., & Rein ten Wolde, P. (2007). Computing stationary distributions in equilibrium and nonequilibrium systems with forward flux sampling. *J Chem Phys*, *127*(11), 114109.

van Erp, T., Moroni, D., & Bolhuis, P. (2003). A novel path sampling method for the calculation of rate constants. *J Chem Phys*, *118*(17), 7762–7774.

Vekilov, P. G. (2004). Dense liquid precursor for the nucleation of ordered solid phases from solution. *Crystal Growth & Design*, *4*, 671–685.

Volmer, M., & Weber, A. (1926). Keimbildung in Übersättigten Gebilden. *Z. Phys. Chem. (Leipzig)*, *119*(227).

Walsh, M. R., Koh, C. A., Sloan, E. D., Sum, A. K., & Wu, D. T. (2009). Microsecond simulations of spontaneous methane hydrate nucleation and growth. *Science*, *326* (5956), 1095–1098.

Wooten, F., Winer, K., & Weaire, D. (1985). Computer generation of structural models of amorphous Si and Ge. *Phys Rev Lett*, *54*(13), 1392–1395.